

## MODELLING AND SIMULATION OF THE PULTRUSION PROCESS WITH CLOSED INJECTION AND IMPREGNATION MOLDS

Renato Bezerra<sup>1</sup>, Frank Henning<sup>2</sup>

<sup>1</sup>Fraunhofer Institute for Chemical Technology ICT, Augsburg Branch Functional Lightweight Design  
FIL, Am Technologiezentrum 2, 86159 Augsburg, Germany

Email: renato.bezerra@ict.fraunhofer.de, Web Page: <http://www.ict.fraunhofer.de/FIL>

<sup>2</sup>Fraunhofer Institute for Chemical Technology ICT, Polymer Engineering Department, Joseph-von-  
Fraunhofer-Straße 7, 76327 Pfinztal, Germany

**Keywords:** Pultrusion, Process simulation, Resin Injection, Curing behavior

### Abstract

In this study, simulation models are developed for the physical processes occurring in pultrusion molds with closed injection and impregnation chambers. Two different mold inlet geometries are studied: a conical tapered inlet and a so called tear drop geometry. The modeled reaction is that of a two-step curing resin system. A commercial software package (Ansys CFX) is applied in the simulation studies. The flow of liquid resin in the injection and impregnation sections is calculated, resulting in predicted pressure and velocity fields within this region. The energy balance equations are solved for the porous (composite) and solid (heated die) domains, with an additional term for the heat generation due to the exothermic reaction. Solving the energy equations yields temperature and degree of cure fields within the die, which are used to calculate resin viscosity and volumetric changes due to thermal expansion and shrinkage due to curing. The pressure variation in the straight die section is obtained from the resin volumetric changes. Simulation results are compared to experimental data from pultrusion processing trials. Experimental data was also used to evaluate the fiber stack distribution within the tear drop die, which is necessary for defining porosity and permeability within the model.

### 1. Introduction

Pultrusion is a mature composite manufacturing technique, in which the fiber reinforcements are usually wetted in a resin bath open to the atmosphere, before being pulled through a heated die. The ease of wetting by this method is contrasted by some inherent disadvantages, such as: limitation of matrix choice to resins of relatively long pot life at room temperature, quality assurance issues, and exposure to volatile chemical components at the working place. These issues are the main drive to development of closed injection and impregnation techniques. Hereby, the resin is injected and reinforcement wetting takes place in a specially designed chamber which is either directly attached to the die, or directly machined as part of a pultrusion die designed for that purpose.

The design of such a die, especially the injection and impregnation cavity, is more complex than that of a standard die. The main reason is that the fiber package must, in this case, be thoroughly wetted with resin while in a compact condition or while being compacted through a short impregnation cavity length up to the die final cross section. Several designs have been proposed over the years in patents and publications [1-4]. The design development of such dies has been performed in most cases in combination with extensive experimental testing by “trial and error” in an extensive time and man-power demanding process. Designs actually implemented by the industry are normally kept undisclosed as company’s internal know-how.

The goal of this work is therefore to get insight and a better understanding of the physical processes undergone in pultrusion molds with closed injection and impregnation. The physical processes involve resin flow through the fiber bed while being compacted, heat transfer between material and mold, and resin curing reaction (coupled with changes in the material state and release of exothermic reaction heat). In order to achieve this, material parameters of resin and fiber reinforcement are experimentally determined, and a geometrical model of the pultrusion mold is generated and translated to a mesh of volume elements. The material parameters and model are then fed to a Computational Fluid Dynamics (CFD) commercial software package (Ansys CFX) and the process is simulated. The simulation yields a resin flow field and the infiltration through the fiber bed, as well as pressure and temperature profiles in the mold cavity. Simulation results are compared to real process conditions in order to evaluate the suitability of the simulation models.

## 2. Materials and methods

In this section the material parameters and the basic assumptions applied in the simulations are discussed. The resin applied to all trials is a two-step curing resin formulation, which cures only partially to a B-stage state within the pultrusion die. The resin formulation is based on the resin named Daron ZW 015864 (Aliancys, Zwolle, Netherlands). A number of additives is added to the formulation, as described in [4, 5]. The b-staging reaction has a relatively short pot life at room temperature (approx. 15 min), which makes the processing through a conventional open bath pultrusion technique unfeasible. The resin was characterized and prediction models were obtained for the kinetic reaction and viscosity evolution in previous work [4, 5]. Glass fiber roving stacks were also characterized in terms of their permeability in a previous study [6]. Pultrusion experimental trials were conducted with two dies having different injection and impregnation chamber designs, namely a conical tapered design and a so called tear drop design. Finally, the strategy applied to the simulations is presented.

### 2.1. Resin curing behavior

A prediction model for the resin curing behavior was developed from differential scanning calorimetry (DSC) data. Data fitting was achieved using the software NETZSCH Kinetics 3.1. The best fit was obtained for a model composed of three reactions steps in sequence. The overall degree of cure  $\alpha$  is given by the weighted sum of the  $\alpha_i$  terms according to Equation 1. The term  $FR_i$  is the fraction of the reaction step  $i$  relative to the total reaction. Since DSC analysis is based on developed exothermic heat of reaction,  $FR_i$  is related to the contribution of reaction  $i$  to the overall degree of cure and to the total heat of reaction  $H_R$ . The volumetric internal heat generation term  $\dot{q}$  is given by Equation 1.

$$\dot{q} = \rho H_R \frac{d\alpha}{dt} = \rho H_R \left( FR_1 \frac{d\alpha_1}{dt} + FR_2 \frac{d\alpha_2}{dt} + FR_3 \frac{d\alpha_3}{dt} \right) \quad (1)$$

where  $\rho$  is the resin density. Figure 1 shows plots of the degree of cure evolution for a series of isotherms.

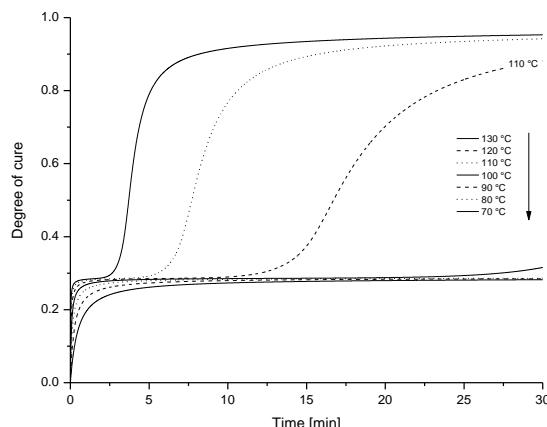


**Figure 1.** Degree of cure evolution of resin system applied in this study for a series of isotherms between 70 and 130 °C.

The B-staging reaction is described by reaction step 1, while the radical polymerization is described by simultaneously occurring steps 2 and 3.  $FR_1$  describes, therefore, the percentage of the total degree of cure relating to the B-staging step. The calculated value was  $FR_1 = 0.29$ , and can be detected by the plateau observed in the lower temperature isotherms depicted in Figure 1. Analysis of this plot gives insight into the processability of the studied formulation to a B-stage during pultrusion. Assuming no substantial temperature increase due to the exothermic heat releases in the first reaction step, one can evaluate for example a die temperature set point of 100 – 110 °C as safe for pultrusion processing, with a time span of approx. 10 min before the second reaction is triggered.

The viscosity evolution during curing was characterized by measurements in a rheometer with a disc-plate configuration in oscillation mode [5]. The software OriginPro was used for data regression. It can apply non-linear fitting of data to a user-defined equation. The Levenberg-Marquardt algorithm is used to adjust the parameter values in an iterative fitting procedure. The data was fitted to the model proposed by Castro and Macosko [7] (Equation 2).

$$\eta = \eta_{\infty} \exp\left(\frac{E_{\eta}}{RT}\right) \cdot \left(\frac{\alpha_g}{\alpha_g - \alpha}\right)^{A+B\alpha} \quad (2)$$

where  $\alpha_g$  is the degree of cure at the gel point and  $\eta_{\infty}, E_{\eta}, A$  and  $B$  are empirical constants. The gel point was determined from the cross-over of the curves of storage and loss moduli to be close to the B-stage plateau at a degree of cure of 0.25.

## 2.2. Permeability of the fiber stack

The in-plane permeability of a roving fiber bundle was experimentally determined using the method described in [6]. It is assumed that the permeability in the out-of-plane direction is the same as the in-plane permeability, the direction transverse to the fiber orientation. The permeability function of fiber volume content was obtained by the model proposed by Gebart [8] considering a quadratic fiber packing and effective fiber diameters of 46  $\mu\text{m}$  in the longitudinal and 13.5  $\mu\text{m}$  in the transverse direction.

### 2.3. Pultrusion trials with closed injection dies

In order to obtain experimental data to compare to processing simulation results, a series of trials was conducted using two pultrusion dies with closed injection and impregnation chambers. The first design (cross section 90 x 4 mm<sup>2</sup>) is based on the descriptions provided by Brown's patent [1]. This die design is referred to as conical. The second die (cross section 180 x 2.45 mm<sup>2</sup>) was designed according to Koppernaes [2] and is referred to in this study as tear drop. Schematic drawings of both dies are shown in Figures 2 and 3.

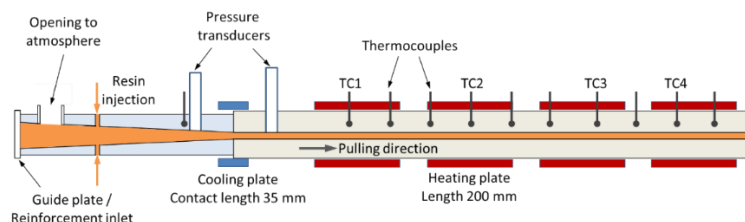


**Figure 2.** Schematic representation of die assembly with conical inlet geometry (not to scale).

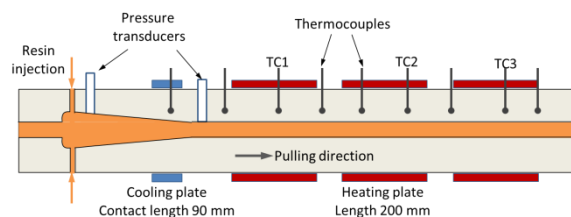


**Figure 3.** Schematic representation of die assembly with tear drop inlet geometry (not to scale).

Trials were conducted with each die and glass fiber roving stacks for a nominal fiber volume content of 64% vol. The resin formulation was processed by mixing and injecting with a metering and mixing machine based on precision gear pumps [4]. The temperature along the curing section of both dies was set to 100 °C for all heating zones. The position of control thermocouples (TC) and heating plates (nominal power 1000 W) can be seen in Figures 2 and 3. The pulling speed was set to 0.3 m/min.

Processing data obtained include: (a) temperatures of control and monitoring TCs at different positions of the metal die, (b) electrical power in percentage of the nominal heating power of each zone, (c) temperature evolution curves within the profile measured by wire TCs fed through the die and (d) liquid resin pressures at the injection and beginning of curing section.

In the conical die, the distribution of the reinforcement fibers in the injection and impregnation chamber can be geometrically approximated by the tapered inlet geometry. In contrast, the distribution of the fiber stack in the injection and impregnation region of the tear drop die is unknown. After passing through the inlet region, the fibers are stretched while in a region with much larger volume filled with resin. Stretching is a result of the pulling action exerted by the machine and the resistance produced by friction when passing through the guiding plates and die inlet cross section. The actual thickness distribution of the fiber stack is an important input parameter for simulation purposes, as it defines the porosity and thus the local permeability of the stack.

In order to evaluate the fiber distribution within the injection region, samples of the whole region were obtained by forcing a sudden process shut down. The pulling process and the injection were stopped at the same time, and heating plates were fastened over the chamber to induce curing of the resin. The result is a block of cured resin with a similar form of the tear drop chamber and the embedded fiber stack. Samples in the longitudinal (pulling) and in the transverse direction were cut and evaluated by optical microscopic analysis. The results of the measured fiber stack thickness along the injection section length are plotted in Figure 4(b). The stretched fiber stack has a nearly constant thickness of approx. 4.7 mm up to the position where the tapering has the same height. From this point on, the fiber stack is compressed along the tapered cavity similarly to the conical die.

## 2.4. Modelling strategy

A commercial software package (Ansys CFX 14.0) is applied for simulation studies. The geometric design and meshing are implemented in the Ansys Workbench tool. Two different models were developed for the two dies. The conical die was designed as a quasi 2D model, i.e. a thin geometric model with one volume element in the thickness. The tear drop die was designed as a 3D model. Taking into account the die symmetry,  $\frac{1}{4}$  of the geometry was designed. The die body is set as a solid domain, and the region of fibers + resin is set as a full porous model, in which the thermal conductivity of the solid and heat transfer between solid and fluid are included in the energy balance.

The porous model supports the definition of two permeability parameters: one in the streamwise direction ( $K_1$ ), defined in this study as the x-axis (and pulling direction), and one in the transverse directions ( $K_2$ ). The distribution of porosity and permeability along the injection sections of both dies is shown in Figure 4. In the tapered section, the porosity and consequently the permeabilities vary according to the position along the x-axis. The model for the conical die assumes that the fibers are uniformly distributed in the thickness direction. The distribution in the tear drop die is based on the fiber stack thicknesses along the injection section as measured from micrographs.

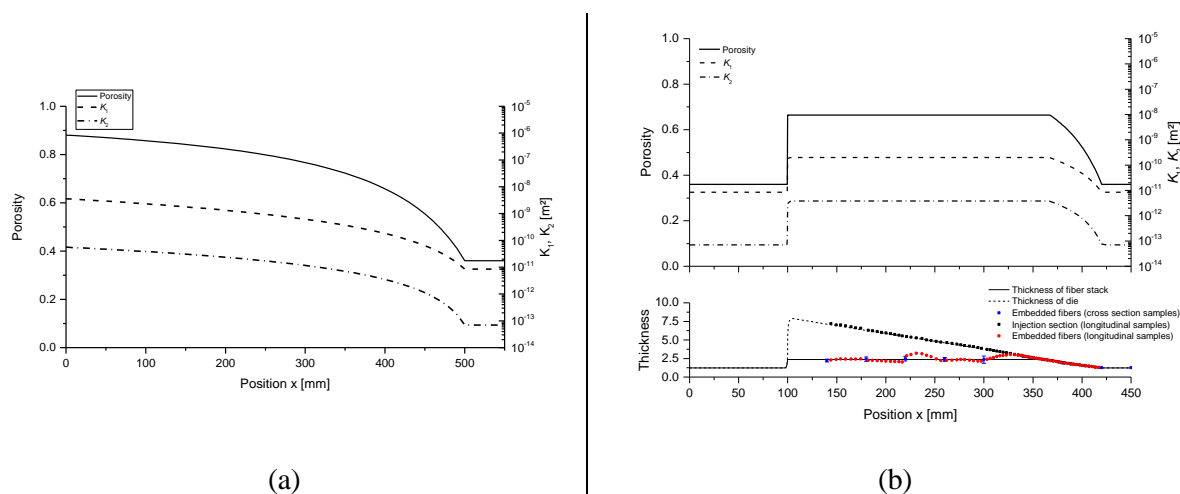


**Figure 4.** (a) Porosity and permeability coefficients as a function of the x position in the tapered region of the conical die; (b) Top: Porosity and permeability coefficients in the inlet region section of the tear drop die. Bottom: Results from microscopic dimensional analysis on longitudinal and cross section samples embedded with a glass fiber stack.

The curing reaction is implemented by means of an additional variable (the degree of cure  $\alpha$ ) in Ansys CFX. It is treated by the solver as a non-reacting scalar component that is transported through the

fluid. Two source terms in the liquid part of the porous domain are associated with this additional variable: the equation change of  $\alpha$  itself, and an energy source, given by Equation 1.

With the calculated local degree of cure, the local resin viscosity can be obtained from Equation 2. However, solving becomes unstable when a high viscosity value is set, since the solving algorithm is optimized for turbulent flow regimes of low viscosity liquids and gases. In order to overcome instability issues during calculations, viscosity is defined as the minimum between the value calculated by Equation 2 and 10 Pa.s.

The simulation results of the CFX model are the pressure and velocity fields in the injection and impregnation regions, as well as the temperature and degree of cure evolution in the curing sections. In order to obtain the pressure evolution in the straight die section, a solving algorithm for calculating the stress-strain evolution as a function of temperature and degree of cure in a 2D field was implemented, following the finite difference discretization method proposed by Bogetti and Gillespie [9] and recently applied to pultrusion process simulations by Baran et al. [10]. The simulation code was written in the Wolfram language (Mathematica 9).

### 3. Results and discussion

Figure 5(a) shows a comparison of measured temperatures and the simulation results of the conical die. The bars located closed to the x-axis reflect the positions of the die cooling and heating zones. Good agreement is found between the measured temperature evolution and the simulation results. Some discrepancy is observed near the peak exotherm, as the predicted temperature increases faster than the experimental results. Towards the downstream section there is another slight temperature increase in the fourth heating zone, which is also not well captured by the simulation. The simulations were conducted by applying a constant heat flux input in each zone and setting a constant Thermal Contact Resistance (TCR) of 0.005 m<sup>2</sup>.K/W between the porous and solid domains throughout the die length. According to Baran et al. [11], a better agreement can be obtained by locally changing the TCR along the die by means of an optimization procedure.

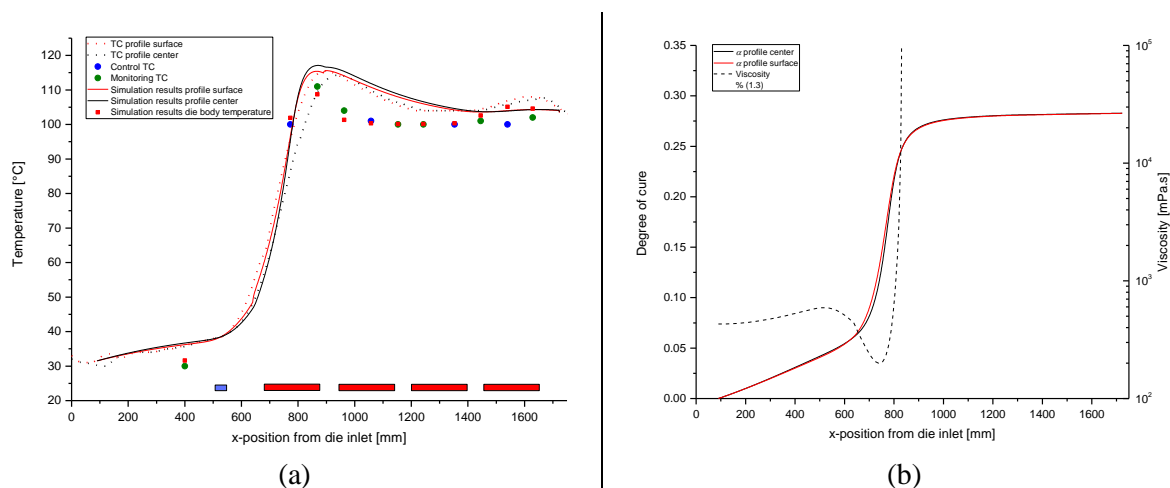


**Figure 5.** (a) Temperatures in the die and pultruded profile as a function of the x position in the conical die; (b) Plots of calculated degree of cure and viscosity along the conical die.

Figure 5(b) shows the calculated degree of cure and viscosity evolution for the conical die. A considerable portion of the reaction already takes place in the conical region, as can be seen by both the increasing temperatures, as well as in the predicted degree of cure. By the end of the conical

section ( $x = 500$  mm) approx. 5% conversion is reached. However, viscosity remains low (under 1 Pa.s) within the length of the conical region, which is a decisive factor for stable processing. Furthermore, a stable processing to a B-stage product is reached, since the degree of cure approaches a plateau at approx. 30% conversion, yet not triggering the second reaction step.

Figure 6 shows plots of pressure rise curves obtained by simulation of both die models. A good agreement with experimental values can be recognized. The discrepancy found for the pressure transducer 1 of the conical die (Figure 6(a)) is due to the actual distribution of the fiber bundles not being uniform as modelled, but rather assembled in bundles. This distribution leaves comparatively more space and less resistance for resin flow around the bundles.

For the simulation of the tear drop die, an inlet boundary condition of 1.3 bar constant pressure was set, corresponding to the measured value of pressure transducer 1. The centerline pressure remains practically constant along the injection region up to the point where the fiber stack is compressed towards the end of the tapered region (see figure 6(b)). The predicted pressure level at the end of the tapered section is slightly larger than measured. This is possibly caused by deformation of the die cavity under liquid pressure, causing variations in the effective local fiber volume content and consequently in the flow regime.

The slight pressure increase in the straight curing sections of both dies is due to a thermal expansion of the composite before the cure shrinkage reverts the process, leading to a detachment of the profile from the cavity wall. Therefore, the pressure curve is shown only up the point where shrinkage surpasses the thermal expansion effect.

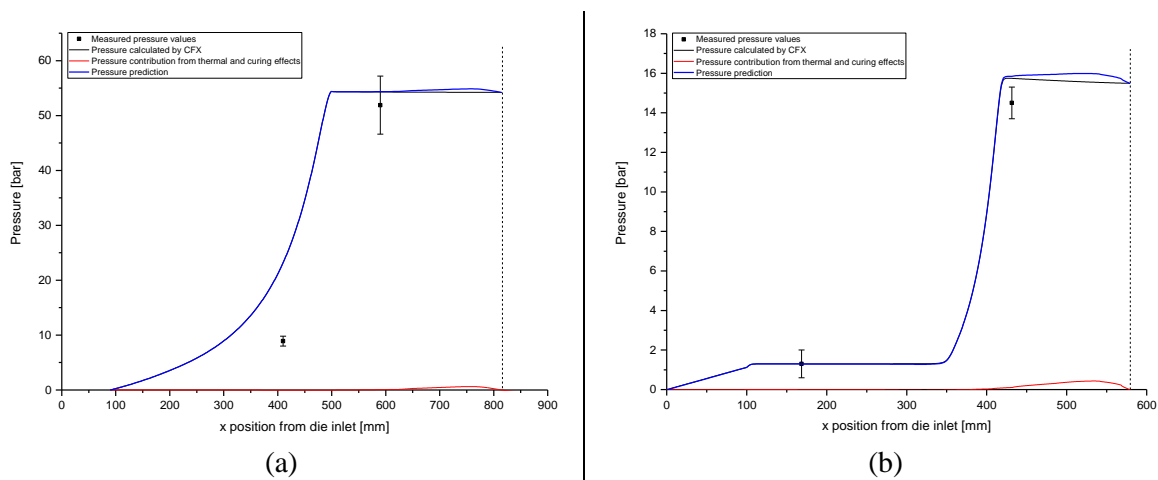


**Figure 6.** (a) Predicted pressure distribution along the conical die length up to detachment point; (b) Predicted pressure distribution along the tear drop die length up to detachment point.

#### 4. Conclusions and outlook

A CFD model for the flow and curing evolution of resin within a pultrusion die was developed using the commercial software Ansys CFX. Two different die designs were modelled. The model is complemented by a 2D finite difference algorithm that calculates pressure variations in the straight die section due to thermal expansion and resin curing shrinkage. The model was applied to simulate the processing of a two-step curing resin, which only partly reacts in the pultrusion die to reach a B-stage condition. Good agreement was found between experimental data and simulation results.

The simulation model also calculates local velocity fields, which may be useful to identify stagnation

regions and assist in die design optimization. Indeed, during long trials (over 2 hours) with the tear drop die, a deterioration of profile quality can be observed due to clogging of the chamber with B-stage material. This particular die design is therefore unsuitable for the stable processing of the resin formulation applied in this study. Beside the velocity fields in steady state, a transient simulation might indicate regions with long residence time, where the resin starts to gel.

## Acknowledgments

This research and development project was partly funded by the German Federal Ministry of Education and Research (BMBF) within the Framework Concept "Research for Tomorrow's Production" (funding number 02PJ2035) and managed by the Project Management Agency Karlsruhe (PTKA). General start-up of the project group, facilities and key technology equipment in Augsburg was funded by the Region of Bavaria, City of Augsburg, BMBF and the European Union (in the context of the program "Investing In Your Future" – European Regional Development Fund). The authors are responsible for the contents of this publication.

## References

- [1] R. J. Brown, S. Kharchenko, H. D. Coffee and I. Huang, "System for producing pultruded components". United States Patent 8,597,016, 2013.
- [2] C. Koppernaes, S. G. Nolet and J. P. Fanucci, "Method and apparatus for wetting fiber reinforcements with matrix materials in the pultrusion process using continuous in-line degassing". United States Patent 5,073,413, 1991.
- [3] S. Li, L. Xu, Z. Ding, L. J. Lee and H. Engelen. Experimental and Theoretical Analysis of Pulling Force in Pultrusion and Resin Injection Pultrusion (RIP)-Part I: Experimental. *Journal of Composite Materials*, 37(2):163-189, 2003.
- [4] R. Bezerra, F. Wilhelm, S. Strauß and H. Ahlborn. Manufacturing of complex shape composite parts through the combination of pull-braiding and blow moulding. *Proceedings of the 20th International Conference on Composite Materials ICCM-20*, Copenhagen, Denmark, July 19-24 2015.
- [5] A. Chaloupka, R. Bezerra, V. Madaksira, I. Taha and N. M. Rudolph. Detection and Modelling of thermal and rheological transitions of a 2-step-curing thermoset using dielectric and standard measuring techniques. *Proceedings of the 20th International Conference on Composite Materials ICCM-20*, Copenhagen, Denmark, July 19-24 2015.
- [6] R. Bezerra, F. Wilhelm and F. Henning, Compressibility and permeability of fiber reinforcements for pultrusion. *Proceedings of the 16<sup>th</sup> European Conference on Composite Materials ECCM16*, Sevilla, Spain, June 25<sup>th</sup> 2014.
- [7] J. M. Castro and C. W. Macosko, Studies of mold filling and curing in the reaction injection molding process. *AIChE Journal*, 28(2):250–260, 1982.
- [8] B. R. Gebart, "Permeability of Unidirectional Reinforcements for RTM," *Journal of Composite Materials*, 26(8): 1100-1133, 1992.
- [9] T. A. Bogetti and J. W. Gillespie, "Process-Induced Stress and Deformation in Thick-Section Thermoset Composite Laminates," *Journal of Composite Materials*, 26(5): 626–660, 1992.
- [10] I. Baran, C. C. Tutum, M. W. Nielsen and J. H. Hattel, "Process induced residual stresses and distortions in pultrusion," *Composites Part B: Engineering*, 51: 148–161, 2013.
- [11] I. Baran, C. C. Tutum and J. H. Hattel, "The effect of thermal contact resistance on the thermosetting pultrusion process" *Composites Part B: Engineering*, 45: 995–1000, 2013.